

# Smartphone-Based Refractive Index Sensor Utilizing Gold Nanorod-Coated CD Grating

Isara Wongsaroj<sup>1</sup>, Chokchai Puttharugsa<sup>2</sup>, and Nongluck Hounkamhang<sup>1,3,\*</sup>

<sup>1</sup> College of Materials Innovation and Technology, King Mongkut's Institute of Technology Ladkrabang, Bangkok, 10520, Thailand

<sup>2</sup> Department of Physics, Faculty of Science, Srinakharinwirot University, 114 Sukhumvit23, Wattana, Bangkok 10110, Thailand

<sup>3</sup> King Mongkut Chaokhunthahan Hospital, King Mongkut's Institute of Technology Ladkrabang, Bangkok, 10520, Thailand

Received: 15 February 2024, Revised: 20 June 2024, Accepted: 23 June 2024

## Abstract

The refractive index measurement device utilizing a gold nanorods (GNRs)-coated CD grating and operated through a smartphone has been developed and demonstrated. The GNRs were synthesized using the seed-mediated growth method, with varying amounts of silver nitrate, specifically tailored for refractive index sensing applications. Due to their anisotropic shapes, GNRs exhibit two absorption peaks associated with localized surface plasmon resonance. This study shows the absorption sensitivity of GNRs changes with refractive index of the solution. Solutions with diverse refractive index values were prepared and measured using the GNRs-coated CD grating as the sensing material and a smartphone as the detector. The observed adsorption changes correlated directly with the refractive index of the solutions. The GNRs-coated CD grating provide higher sensitivity when compared with uncoated CD grating. Remarkably, this setup eliminates the need for traditional optical components, relying solely on the smartphone's LED flash and camera. This work demonstrates the potential for portable, cost-effective, and easily deployable refractive index sensing devices.

**Keywords:** Gold nanorods, Refractive index sensor, CD grating, Surface plasmon resonance

## 1. Introduction

Surface plasmon resonance (SPR) occurs when an electromagnetic wave excites the free electrons at a metal-dielectric interface under specific conditions that match the oscillation frequency of the surface conduction electrons in the metal. This phenomenon is typically observed through diffraction gratings and prism couplers. The SPR effect manifests as either a dip in the reflectance spectrum or a peak in the absorbance spectrum of the electromagnetic wave. This spectral response is sensitive to changes in the refractive index of the surrounding medium [1]. Localized surface plasmon resonance (LSPR) typically involves metallic nanoparticles, as it arises when the frequency of incident photons matches the collective oscillation frequency of conduction electrons within these nanoparticles [2], [3]. Gold nanorods (GNRs) are commonly employed in LSPR investigations because of their distinctive optical characteristics. GNRs possess anisotropic shapes, manifesting two absorption peaks corresponding to LSPR. These peaks arise from electron oscillations along the long and short axes of the GNRs, termed as the longitudinal surface plasmon resonance (l-SPR) and the transverse surface plasmon resonance (t-SPR) [4], respectively.

The LSPR characteristics of GNRs significantly rely on factors such as their size, shape, dielectric properties, and the composition of the surrounding medium [5]. The seed-mediated growth method is commonly employed in the synthesis of gold nanorods due to its ability to produce high-quality and high-yield GNRs. Adjusting the amount of silver nitrate ( $\text{AgNO}_3$ ) during the synthesis process can result in higher aspect ratios of the GNRs [6].

Smartphones come equipped with a range of features including Wi-Fi, Bluetooth, high-resolution cameras, multimedia capabilities, and a variety of built-in sensors like gyroscopes, ambient light sensors (ALS), and GPS. With the rapid advancements in both hardware and software, smartphones now boast computational power comparable to that of desktop computers, marking a significant evolution in their

capabilities. Currently, a wide array of sensing devices has emerged, integrating optical technologies with smartphones for biosensing purposes. These devices rely on measuring parameters such as transmitted intensity, color changes, reflectivity changes, image, and fluorescence intensity. Notably, optical imaging and sensing techniques leveraging smartphones have garnered significant interest due to their ability to circumvent the requirement for bulky and expensive optical instrumentation, all while maintaining high sensitivity and image resolution [7]. In 2022, Carlos Angulo Narrios [8] has demonstrated a smartphone optical platform for measuring the refractive indexes of fluids based on a DVD grating. Refractive index (RI) resolution can be translated to a grating depth resolution smaller than typical biomolecule layer thicknesses, which supports the suitability of the proposed platform for label-free biosensing based on monitoring diffraction efficiency changes due to affinity binding events on the grating surface. To the use of low-cost DVDs, should contribute to the implementation of cost-saving optical designs for in-field applications.

In this work, we studied the characteristics of a CD grating as a RI transducer by comparing its sensitivity to refractive index changes when coupled with a smartphone. The smartphone's LED flash functions as a light source, and the light incident on the CD grating is diffracted. The smartphone camera captures this first-order diffracted light. To make a comparison with uncoated CD grating, GNRs were synthesized and coating on the same structure of a CD grating to fabricate GNRs-coated CD grating. The sensitivity study was performed by testing the sensor with solutions of different refractive indices and collecting the intensity of the first-order diffracted light signal to construct a calibration curve.

## 2. Materials and methods

### 2.1 Synthesis of GNRs

The GNRs stabilized with cetyltrimethylammonium bromide (CTAB) were synthesized using the seed-mediated growth method [6]. For seed solution, Gold (III) chloride hydrate ( $\text{HAuCl}_4$ ) solution (5 mL, 0.00025 M) was added into CTAB solution (5 mL, 0.2 M) under magnetic stirring. The freshly prepared sodium borohydride ( $\text{NaBH}_4$ ) solution (0.6 mL, 0.01 M) at 0 °C was then added quickly. The solution was stirred for 2 min and then aged for 2 h at 30 °C before use. Subsequently, the growth solution was prepared by mixing  $\text{HAuCl}_4$  solution (5 mL, 0.0005 M),  $\text{AgNO}_3$  solution (0.004 M) and CTAB solution (5mL, 0.0005M). L-ascorbic acid solution (70  $\mu\text{L}$ , 0.0788 M) was then added to reduce the gold salt. The seed solution (12  $\mu\text{L}$ ) was added to the mixed solution and allowed to stand at 30 °C for 24 h. Finally, the solution was centrifuged (10,000 rpm, 25 C, 10 min) and washed 2 times with Deionized (DI) water, and then the precipitation was dispersed into DI water to obtain the GNR solution. DI water was used for all preparations.

### 2.2. Characterization of GNRs

The absorption of gold nanorods solution was tested by UV-VIS spectrophotometer (Thermo Scientific, Orion AquaMate 8000). The size distribution of the gold nanorods was determined using a Beckman Coulter Delsa Nano C particle analyzer, which employs Dynamic Light Scattering (DLS) technique to measure the size distribution of particles in the nanometer range. The measurement was performed three times to obtain an average value.

### 2.3 Refractive index sensor

surface plasmon resonance (SPR), a sensitive technique used to detect changes in the refractive index of a medium by monitoring the resonance conditions at the interface between a metal and a dielectric material. SPR occurs when the wave vector of incident light matches the wave vector of surface plasmon resonance at the interface between a metal and a dielectric material. This alignment excites the SPR effect, which is highly sensitive to changes in the dielectric properties of the surrounding medium. The refractive index sensor we developed utilizes a grating structure to facilitate this excitation through light diffraction, enabling precise measurements of refractive index changes.

When the wave vector  $k_0$  of incident light along the reflecting interface is equal to the wave vector of surface plasmon resonance ( $k_{spr}$ ), the SPR effect at the interface between metal and dielectric can be excited. The real part of  $k_{spr}$  can be expressed as equation (1):

$$k_{spr} = k_0 \sqrt{\frac{\epsilon_m \epsilon_d}{\epsilon_m + \epsilon_d}} \quad (1)$$

where  $\epsilon_d$  is the dielectric constant of the analyte, and  $\epsilon_m$  is the dielectric constant of the metal. Since the free space wave vector  $k_0$  is smaller than the SPR wave vector  $k_{spr}$ , a grating structure is necessary to introduce the additional wave vector difference. Therefore, the excitation of surface plasmon is based on the diffraction of light on a grating. In theory, the m-th order diffraction wave vector and the surface plasmon wave of metal grating should satisfy as equation (2):

$$n_d \sin\theta_{SPR} + m \frac{\lambda}{P} = \pm \left( Re \left\{ \sqrt{\frac{\epsilon_m \epsilon_d}{\epsilon_m + \epsilon_d}} \right\} + Re \left\{ \frac{\Delta\beta_g \lambda}{2\pi} \right\} \right) \quad (2)$$

where  $\lambda$  is the wavelength of the incident light,  $\theta_{SPR}$  is the SPR angle, m is the diffraction order, P is the grating pitch,  $\Delta\beta_g$  represents the propagation constant which causes a shift in the wavevector induced by the presence of the grating and  $n_d$  is the RI of the surrounding dielectric medium. [1], [9].

To expose a 50 mm × 20 mm piece from a CD (hp brand) used as a diffraction grating, we first use paper cutter to cut a disc, then gently separate the disc along the metal layer and polycarbonate reflective layer by hand, and then put the side containing the grating structure into the isopropanol to clean the organic dye on the surface. The CD has a continuous groove imprinted on transparent surface, which creates a periodic structure that diffracts light. The high-resolution atomic force microscope (AFM, Seiko Instruments, SPI3800N/SPA400) was used to see the morphology of the surface of CD-grating. Fig. 1 b) show AFM measurements of the CD surface with the groove depth (D) is 69.3 nm and pitch (P) is 1.83 μm.

### 2.4 Refractive index measurement

Sample measurements were conducted in a small chamber constructed by placing the CD grating piece at the bottom and using acrylic foam tape to create a well area for dropping the test solutions, as shown in Fig. 1 a). The solution sample was pipetted and dropped onto this chamber, covering the CD grating's surface. The light from the smartphone's source was incident on the grating, and the diffracted light was monitored and captured as an image displayed on the smartphone. After testing each solution, it was removed from the chamber, and the next higher concentration solution was pipetted and dropped into the chamber for refractive index measurement. To make a comparison with uncoated CD grating, the same structure of a CD grating was incubation in the synthesized GNRs solution overnight to fabricate GNRs-coated CD grating. After that, GNRs-coated CD grating was rinsed with DI water to remove any excess GNRs from the surface. In this experiment, glycerol solutions ranging from 0-20% (v/v) were prepared, corresponding to RI values between 1.3330 and 1.3636. The refractive indices of these solutions, created by diluting glycerol with deionized water, were measured using an ABBE Refractometer (Model 2WAJ, WINCOM, China). Both uncoated and GNRs-coated CD gratings were tested with these glycerol solutions. The RGB intensities of the first-order diffraction light were captured using a smartphone and analyzed with the Image J program. The series of glycerol solutions were added into the chamber, each possessing a volume of 200 μL, with the light intensity spectrum then collected for each solution.

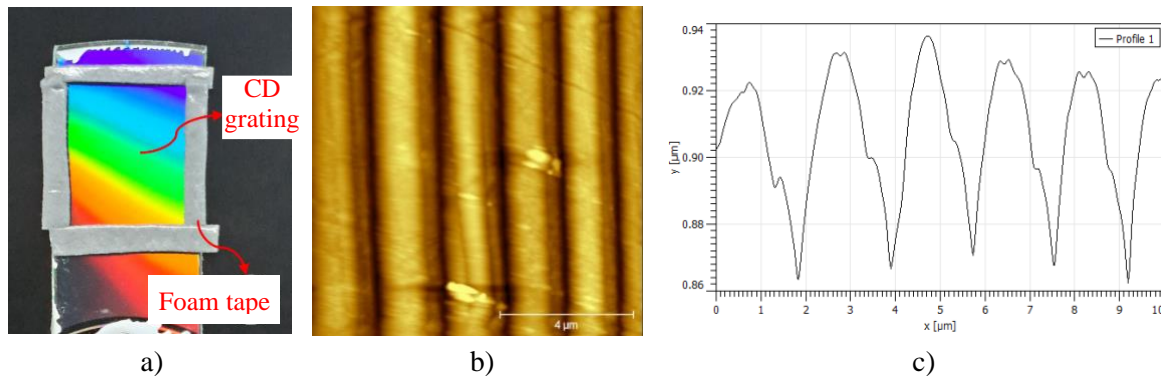


**Fig. 1.** a) Photograph of the CD used as a diffraction grating for RI sensor, b) AFM image, and c) Profile of the surface CD grating

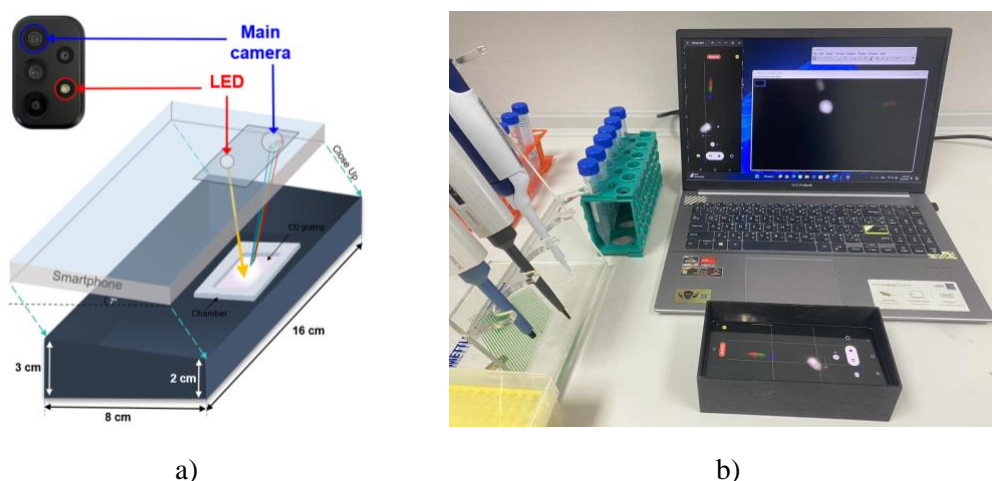


**Fig. 2.** a) Schematic illustration of the smartphone sensing platform, and b) The photograph of the experimental set up with smartphone sensing device and the monitor display

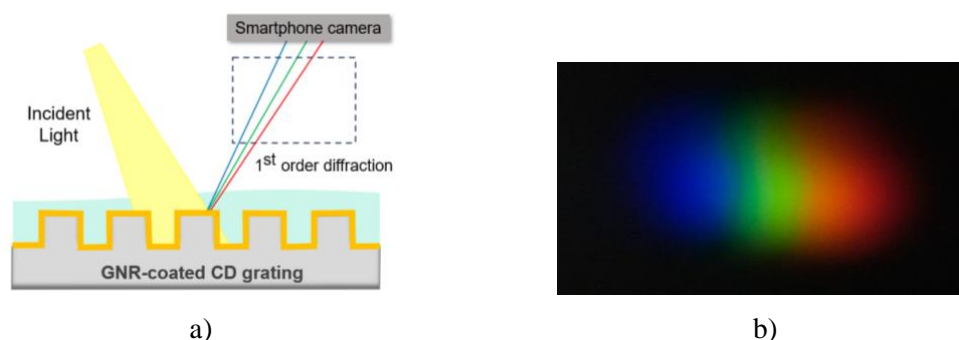


**Fig. 3.** a) Schematic of the refractive index measurement on the grating, and b) Images of reflected of 1<sup>st</sup> order diffracted light

To verify that the GNRs-coated grating we made can excite LSPR, we carried out further experimental research. A smartphone was used for sample interrogation and measurement recording. Fig. 2 a). shows a schematic diagram of the smartphone sensing platform and Fig. 2 b). shows the photograph of the experimental set up with smartphone sensing device and the monitor display. The CD grating was placed 2 cm away from the LED and slightly tilted at an incident angle of  $7^\circ$  in order to image the reflection first-order diffraction pattern. The diffraction intensity depends on the RI of the solution.

Images of the first-order diffracted light captured by the smartphone camera were recorded as JPEG files, as shown in Fig. 3 b). The freeware ImageJ [10] was employed for image analysis. A rectangular area covering the imaged diffraction pattern was selected as the region of interest (ROI). Subsequently, the mean values of red (R), green (G), and blue (B) intensities were calculated and utilized as the sensor response. To determine the sensitivity, the RGB intensities were plotted against the refractive index values, and the slope of the linear relationship was calculated. The sensitivity of the sensor was obtained from these slopes and compared between different gratings.

### 3. Result and discussion

#### 3.1 Optical properties of synthesized GNRs

The seed-mediated growth method was used to synthesis GNRs as a wet chemical reduction due to the simplicity method in structural modifications. It is a widely used technique for synthesis gold nanorods with controlled aspect ratios. This method involves two main steps: (1) the preparation of gold seed solution and (2) the growth of gold nanorods using the seed solution. It's important to note that the specific concentrations of reagents, reaction times, and temperatures may vary depending on the desired

characteristics of the gold nanorods. Proper optimization and characterization of the synthesized gold nanorods are crucial for their successful application in various fields. In this experiment, the small amount of silver nitrate ( $\text{AgNO}_3$ ) solution (50, 80, 110 and 140  $\mu\text{L}$ ) were introduced to the growth solution to control the aspect ratio of the gold nanorods. Characterize the synthesized gold nanorods using UV-vis spectroscopy and dynamic light scattering (DLS) technique to determine their optical properties and size distribution. From Fig.4 a) shows the UV-vis spectrum of gold nanorods which synthesized by different amount of  $\text{AgNO}_3$ . The distinct SPR bands were observed at 511-519 nm which is corresponded to the t-SPR band and at 625-674 nm which is corresponded to the l-SPR band. From the results, the spectra reveal the effect of  $\text{AgNO}_3$  concentration on the aspect ratio of the synthesized gold nanorods. The l-SPR band was shifted to the higher wavelength (red shift) from 625 to 674 nm while the t-SPR band was changed a little bit when increase the amount of  $\text{AgNO}_3$ . This red-shift in the l-SPR peak indicates an increase in the aspect ratio of the gold nanorods as the  $\text{AgNO}_3$  concentration increases. The aspect ratio is the ratio of the length to the width of the nanorods. A higher aspect ratio results in an l-SPR peak at longer wavelengths, while a lower aspect ratio leads to an l-SPR peak at shorter wavelengths.

The role of  $\text{AgNO}_3$  in the synthesis of gold nanorods is to control the growth of the nanorods along the longitudinal axis. Silver ions ( $\text{Ag}^+$ ) adsorb onto the surface of the growing gold nanorods, preferentially binding to the {110} facets on the sides of the nanorods. This selective adsorption slows down the growth of the nanorods along the width, promoting the growth along the length and thus increasing the aspect ratio. [11] The red shift of l-SPR absorption peak indicate the higher aspect ratio of synthesized gold nanorods. As described in previous literature, several studies [12]-[14] have used UV-vis spectroscopy to characterize gold nanorods and estimate their aspect ratios based on the position of the l-SPR peak. By comparing the experimentally obtained UV-vis spectra with theoretical models or previously established [12] correlations, researchers can estimate the aspect ratio of the synthesized gold nanorods with different concentration of  $\text{AgNO}_3$  (50-140  $\mu\text{L}$ ) around 2.0-2.9. These results confirmed that the nanorods is present in the solutions. The gold nanorods synthesized by adding 110  $\mu\text{L}$  was chosen for use in the next experiment due to the highest l-SPR absorption intensity which related to more content of gold nanorod in the solution.

Dynamic light scattering (DLS) measurements, as shown in Fig. 4 b), revealed the presence of two distinct size distributions for the synthesized GNRs. The distinction between the two peaks in the particle size distribution for anisotropic nanoparticles like gold nanorods arises from the different modes of Brownian motion they exhibit in solution. The larger peak at higher dimensions represents the translational diffusion and overall hydrodynamic size of the nanorods due to the fluctuations in scattered light intensity caused by the Brownian motion of particles in solution. While the smaller peak at lower dimensions is associated with the rotational diffusion, which is influenced by the aspect ratio or shape anisotropy of the nanorods which do not directly correspond to the actual size of the nanorods but rather their rotational dynamics.

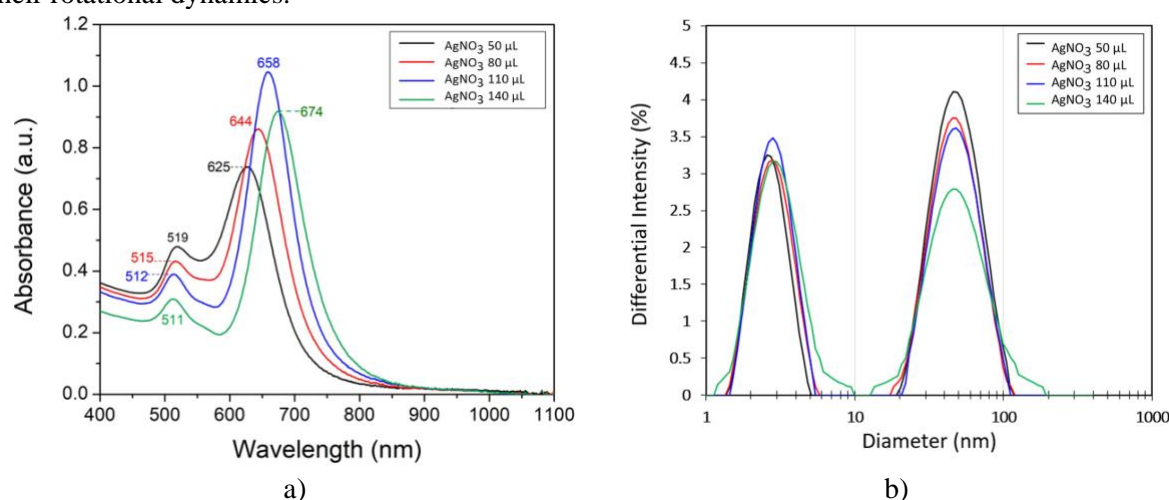


**Fig. 4.** a) Absorbance spectrum, and b) Size distribution of the synthesized GNRs with different amount of  $\text{AgNO}_3$

The results demonstrate the ability to tune the aspect ratio of GNRs by varying the AgNO<sub>3</sub> concentration during synthesis, which consequently shifts the 1-SPR band position. This tuning capability is advantageous for various applications, including refractive index sensing, as the 1-SPR band can be optimized for the desired wavelength range and sensitivity.

### 3.2 Sensitivity test from refractive index measurement

For RI sensors, sensitivity is an important parameter to estimate the property, which can be defined from the slope of the relation between intensity of diffraction light and the RI value. In this experiment, the 0-20% (v/v) glycerol solutions were prepared to obtain the samples with the RI range of 1.333-1.3636. The uncoated grating and GNRs-coated grating were tested with glycerol solutions at different RI values (1.333-1.3636) to compare the sensitivity. It shows that with the increase of RI values, the RGB intensities of the 1<sup>st</sup> order diffraction light become lower as shown in Fig. 5. For binary phase grating, the ratio of the first-order reflection optical intensity to the total incident intensity, or the first-order reflection efficiency ( $\eta$ ), varies with the RI sample ( $n_s$ ) as equation (3), which states that  $\eta$  decreases quadratically with increasing  $n_s$  [8].

$$\eta \propto \left[ \frac{\pi d(n_g - n_s)}{\lambda} \right]^2 \tag{3}$$

where  $d$  is the grating path length (groove depth),  $n_g$  is the grating refractive index and  $\lambda$  is the wavelength of incident light. From equation (3), the  $\eta$  also depended on the path length of the grating therefore, the diffraction efficiency decreases when refractive index of solution increased, and grating path length decreased. The sensitivity of the RI sensor based on RGB intensity measurements from a smartphone detector for both uncoated grating and GNRs-coated grating are observed in Fig. 5 a) and 5 b). The intensity values of all three-color channels (red, green, and blue) decreased linearly as the refractive index increased. However, the GNRs-coated grating exhibited enhanced sensitivity compared to the uncoated grating, as evidenced by the steeper slopes of the linear regression lines for all color channels, indicating that the GNRs-coated grating experienced a larger change in RGB intensity values for the same change in refractive index. Among the three-color channels, the blue channel displayed the highest sensitivity for both grating types, followed by the green channel, while the red channel showed the lowest sensitivity. Moreover, the GNR-coated grating achieved improved linearity and reliability of the sensor response, as demonstrated by the higher R<sup>2</sup> values of the linear regression lines compared to the uncoated grating. Additionally, the GNR-coated grating generally exhibited higher RGB intensity values across the tested refractive index range, potentially due to the plasmonic enhancement effects of the gold nanorods on the optical response.

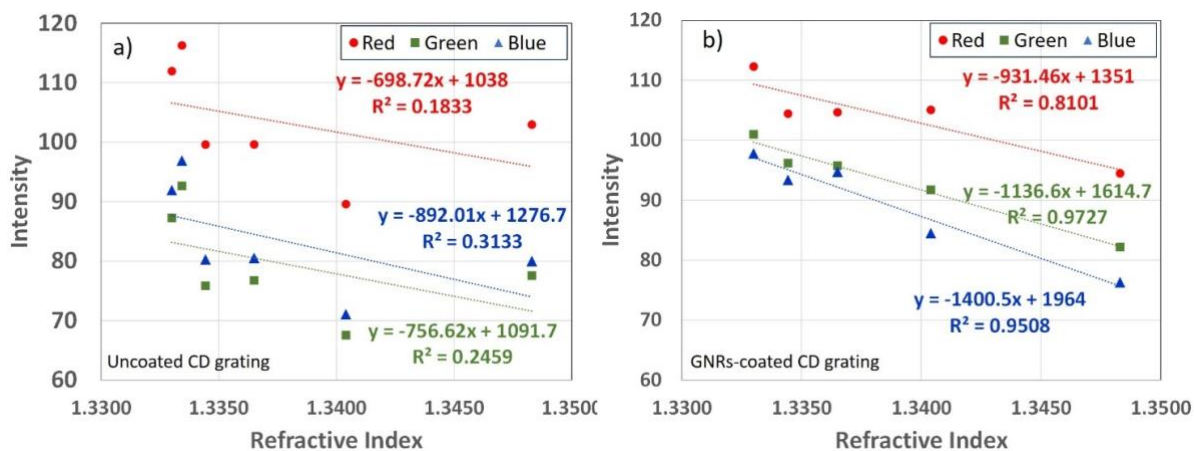


**Fig. 5.** The relation between RGB intensity against the refractive index of a) The uncoated CD grating and b) GNRs-coated CD grating

It is noticeable that the sensitivity of GNRs-coated grating has a good linearity with the increase of the RI compared to uncoated grating. Because of their anisotropic shapes, GNRs display two LSPR absorption peaks. By adjusting the aspect ratio of GNRs, the 1-SPR can be shifted to the visible and near-infrared regions, increasing its sensitivity to variations in the dielectric properties of the surrounding environment. The results in this work show the potential of GNRs-coated CD gratings as sensitive RI sensors, with the smartphone-based RGB intensity measurements providing a simple and accessible method for quantitative analysis.

#### 4. Conclusion

In this research, a smartphone-based refractive index (RI) sensor was developed by integrating gold nanorods (GNRs) with a CD grating. This approach significantly reduces the production costs associated with traditional RI sensors. The fabrication process is straightforward, and the sensor exhibits a linear response, making it suitable for biosensing applications. By monitoring the intensity variations using the smartphone's built-in spectrometer, the need for additional optical components such as lenses, filters, or apertures is eliminated, thereby simplifying the implementation and reducing the overall cost. The LED flash and camera of the smartphone are the only essential components required for this configuration. Furthermore, the sensitivity of the GNRs-coated grating can be fine-tuned by adjusting the dimensions of the GNRs, such as their aspect ratio, enabling the creation of optimized sensors for specific applications in the future. The findings of this study demonstrate the successful integration of GNRs-coated gratings with smartphone technology, paving the way for the development of accessible, sensitive, and cost-effective RI sensing devices.

#### Acknowledgment

The authors acknowledge the facilities, and technical assistance from Nanotechnology and Materials Analytical Instrument Service Unit (NMIS) of College of Materials Innovation and Technology, King Mongkut Institute of Technology Ladkrabang.

#### References

- [1] Su, W., Luo, Y., Ding, Y., & Wu, J. (2021). Low-cost surface plasmon resonance refractive index sensor based on the metal grating in DVD-ROM disc. *Sensors and Actuators A: Physical*, 330, 112858. DOI:10.1016/j.sna.2021.112858.
- [2] Yang, A., Wang, D., Wang, W., & Odom, T. W. (2017). Coherent light sources at the nanoscale. *Annual Review of Physical Chemistry*, 68, 83-99. DOI:10.1146/annurev-physchem-052516-050730.
- [3] Cao, J., Galbraith, E. K., Sun, T., & Grattan, K. T. V. (2011). Comparison of surface plasmon resonance and localized surface plasmon resonance-based optical fibre sensors. *Journal of physics: Conference series*, 307(1), 012050. DOI:10.1088/1742-6596/307/1/012050.
- [4] Pellas, V., Hu, D., Mazouzi, Y., Mimoun, Y., Blanchard, J., Guibert, C., Salmain, M., & Boujday, S. (2020). Gold nanorods for LSPR biosensing: synthesis, coating by silica, and bioanalytical applications. *Biosensors*, 10(10), 146. DOI: 10.3390/bios10100146.
- [5] Pang, R., Zhu, Q., Wei, J., Wang, Y., Xu, F., Meng, X., & Wang, Z. (2021). Development of a gold-nanorod-based lateral flow immunoassay for a fast and dual-modal detection of C-reactive protein in clinical plasma samples. *RSC advances*, 11(45), 28388-28394. DOI: 10.1039/D1RA04404D.
- [6] Nikoobakht, B., & El-Sayed, M. A. (2003). Preparation and growth mechanism of gold nanorods (NRs) using seed-mediated growth method. *Chemistry of materials*, 15(10), 1957-1962. DOI: 10.1021/cm020732l.
- [7] Wang, Y., Liu, X., Chen, P., Tran, N. T., Zhang, J., Chia, W. S., Boujday, S., & Liedberg, B. (2016). Smartphone spectrometer for colorimetric biosensing. *Analyst*, 141(11), 3233-3238. DOI: 10.1039/C5AN02508G.
- [8] Angulo Barrios, C. (2022). Smartphone-based refractive index optosensing platform using a DVD grating. *Sensors*, 22(3), 903. DOI:10.3390/s22030903.

- 
- [9] Singh, G. P., & Sardana, N. (2022). Smartphone-based surface plasmon resonance sensors: A review. *Plasmonics*, 17(5), 1869-1888. DOI:10.1007/s11468-022-01672-1.
- [10] Ferreira, T., & Rasband, W. (2012, 10). ImageJ User Guide. Imagej.net. <https://imagej.net/ij/docs/guide/146.html>.
- [11] Almora-Barrios, N., Novell-Leruth, G., Whiting, P., Liz-Marzan, L. M., & Lopez, N. (2014). Theoretical description of the role of halides, silver, and surfactants on the structure of gold nanorods. *Nano letters*, 14(2), 871-875. DOI:10.1021/nl404661u.
- [12] Orendorff, C. J., & Murphy, C. J. (2006). Quantitation of metal content in the silver-assisted growth of gold nanorods. *The Journal of Physical Chemistry B*, 110(9), 3990-3994. DOI: 10.1021/jp0570972.
- [13] Eustis, S., & El-Sayed, M. A. (2006). Determination of the aspect ratio statistical distribution of gold nanorods in solution from a theoretical fit of the observed inhomogeneously broadened longitudinal plasmon resonance absorption spectrum. *Journal of Applied Physics*, 100(4). DOI: 10.1063/1.2244520.
- [14] Vigderman, L., Khanal, B. P., & Zubarev, E. R. (2012). Functional gold nanorods: synthesis, self-assembly, and sensing applications. *Advanced materials*, 24(36), 4811-4841. DOI: 10.1002/adma.201201690.